Mechanical Characterization of Al/Ti-6Al-4V Surface Composite Fabricated via FSP: A comparison of Tool Geometry and Number of Passes

Adedotun Adetunla, Esther Akinlabi

Department of Mechanical Engineering Science, University of Johannesburg, Johannesburg 2006, South Africa.

Email: Adedotun Adetunla – dotunadetunla@yahoo.com

Abstract

Aluminium alloys specifically the 1100 grade are used majorly in the manufacturing industries. However, the alloy experiences wear while being used which in turn causes reduction in the service life of this alloy. One of the most common causes of failure in aluminum alloy is wear and with the aim to improve the wear resistance of this aluminum alloy, friction stir processing (FSP) is used to fabricate the surface composite of the Al/Ti- 6Al-4V system. The Ti-6Al-4V particles were mixed into the 1100 Al alloy by employing two different tool geometries (i.e, square shape and threaded taper) with a varying number of passes from 1 - 3 passes and a varying tool rotational speed of 600 and 1200rpm. The results of this study show that the tool shape, tool speed and the number of passes play significant role in the distribution of the reinforcing particles, which consequently affect the hardness, microstructural modifications, grain size and wear resistance of these composite samples. The highest wear resistant composite was attained with threaded taper tool with 3 passes at 1200 rpm. Furthermore, the composite realized a wear resistance of 50% increment and a 40% reduction in friction coefficient compare to the 1100 Al alloy, this composite consequently exhibits the highest hardness and strength.

Keywords

Ti-6Al-4V; Microstructures; Composites, Surface Mechanical Properties, Wear

Introduction

The use of friction stir processing (FSP) as a method to develop surface metal matrix composites (MMCs) has become popular in recent year. FSP has a working principle based on friction stir welding (FSW) which was invented in the year 1991 by The Welding Institute (TWI) [1]. The principle of FSP is one in which a non-consumable rotating tool is inserted into the surface of a work piece, the work piece then become softened without reaching its melting point due to the heat produced by the stirring process [2]. This work piece experiences intense plastic deformation and consequently modifies its microstructure, the microstructural modifications and dynamic recrystallization which occur at the stir zone of the FSPed sample creates high angle grain boundaries with equiaxed ultrafine grain sizes. Several studies have reported FSP as means to modify the microstructure in different alloys [3]–[5]. Furthermore, it has been reported in some recent studies to have improved the wear performance and mechanical properties of different aluminum alloys [4], [6], [7].

Aluminium alloys are welded easily with good formability, it has been proven that they have high strength to weight ratio, high thermal conductivity and also exhibit high ductility [8]. These properties increased the applicability of Al alloys to wide range of industries such as in the aerospace, marine, plastics industries and automobile. Contrarily, Al and its alloys exhibit poor abrasion properties and low wear resistance even though they possess high strength to weight ratio and good strength [9]. Recent studies show that Aluminium alloys can exhibit better hardness, good mechanical properties and better wear resistance by reinforcing the surface with ceramic particles[10]–[12]. However, these reinforced alloys suffer loss of toughness and ductility due to the addition of the particles which sometimes serve as inclusion and contaminations[13].

Many investigations have been carried out to prepare surface composites such as Al/SiC[[14] and Al–Mg–Si/TiB2[15]. Furthermore, intermetallic composites have also been produced via FSP like Al-Fe and Al-N with an appropriate grained Al matrix [16]. Additionally, FSP has been employed for the production of hybrid composites like Al/SiC- Al2O3[17], this process is done by adding two or more types of reinforcement to strengthen the metal matrix which result to better properties than those strengthened with one reinforcement powder. Al metal matrix composites are usually strengthened by various ceramic particles such as $ZiSiO_4$, B_4C, AlN, SiC and TiC [15]–[20]. The most commonly used titanium alloy is Ti-6Al-4V, which is an $\alpha + \beta$ alloy[24]. The Ti-6Al-4V alloy has been created for aerospace applications to produce better mechanical properties while maintaining the corrosion resistance [25]. This alloy

exhibits improved wear characteristics, lubrication and friction in comparison to pure titanium [26], the Ti-6Al-4V nanoparticles have also been produced for better toughness [27].

Vijayavel et al investigated the effect of tool pin in fabricating Aluminium based metal matrix, the microstructure and tensile properties were considered, the report shows that the tool pin profile plays an important role in the formation occurring at the stir zone [28] Numerous studies [29]–[31] have indicated that the properties of the FSP composite sample is affected by adequate mixture of the reinforcing particles in the base material, and this mixture is dependent on the tool speed, tool geometry and number of passes employed. Hence, this study aim to attain the best combination of these parameters to produce better wear resistance, higher hardness and uniform distribution of the reinforcement particles within the Al alloy matrix. No other study has attempted to reinforce 1100 Al alloy with Ti-6Al-4V by considering the effect of various tool geometries and number of passes on its wear behaviour, microstructure and hardness of the composites samples. The results obtained in the current study are presented and discussed in detail.

Experimental

1100Al as base sheet and Ti-6Al-4V as reinforcement element are the materials used in this research. The powder size of the Ti-6Al-4V element was found to be 35 nm in size, the chemical composition of this powder is shown in Table 1 while Table 2 presents the chemical composition of the as-received 1100 Al alloy. Fig 1a shows the SEM analysis of the Ti-6-Al- 4V powder, the powder's structure is non-porous and spherical, which has satellites joined with the bigger particles, the presence of these satellites show that the Ti 6Al-4V powder was produced through gas atomization. The microstructure of the as-received 1100 Aluminium is shown in Fig 1b. The dark particles (precipitates) in the as-received sample indicates a continuous distribution inside the grains and also within the grain boundaries, the cell format of these precipitates are eutectic. Other elements were also found in this alloy which are indicated as "others" in Table 2, these elements are seen to be carbides and oxides as a result of inclusions and impurities associated with the preparation process of the 1100 Al alloy.

Table1: Chemical Composition of Ti-6Al-4V

Element	Ti	C	Fe	N	Al	O	V
Weight(%)	89.18	0.08	0.03	0.06	6.25	0.20	4.2

Table2: Chemical composition of the 1100 Alloy.

Element	Al	Cu	Zn	Fe	Si	Others
Percentage	97%	0.15%	0.09%	0.95%	0.95%	0.86%

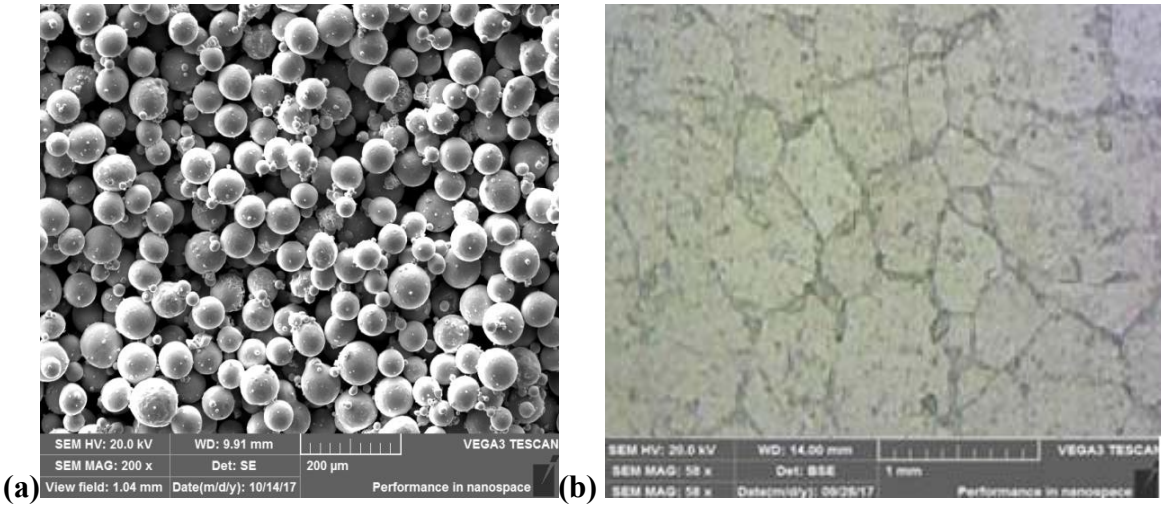

Fig 1: (a) SEM analysis of the Ti-6Al-4v (b) SEM analysis of the 1100 Al

Figure 2a shows the experimental setup used for FSP of the Al/Ti-6Al-4V system, the 5-axis friction stir welder machine has 12 HP spindle motor with 50KN plunge load and 3500rpm turn speed capacity. The sheet thickness of 5 mm was cut to a measurement of 250 x 200 mm in a rectangular form, and it has four grooves with 3.5 mm width and 3 mm depth cut all through the top surface of these aluminium sheets. Some studies show that the volume fraction of reinforcing powders will affect the properties of the FSP samples fabricated and it has been proven that 20% to 25% volume of the reinforcing particles can adequately strengthen the base metal [32]. Therefore, 25% volume of Ti-6Al-4V particles was deposited into the groove and the calculation was done based on assertion of Thangaarasu et al [33], by using the following formula:

$$Volume\ fraction = (Area\ of\ groove \div Area\ of\ surface\ composite) \times 100.$$

$$Area\ of\ grooves = (Groove\ width \times Groove\ depth)$$

A pinless tool was employed to close the grooves in order to avoid wasting the Ti-6Al-

4V powder deposited inside the grooves. Therefore, the surface of these aluminium sheets were subjected to multi pass FSP with 100% overlap, a crown appearance of the aluminium sheet that has been worked on is shown in Figure 2b.

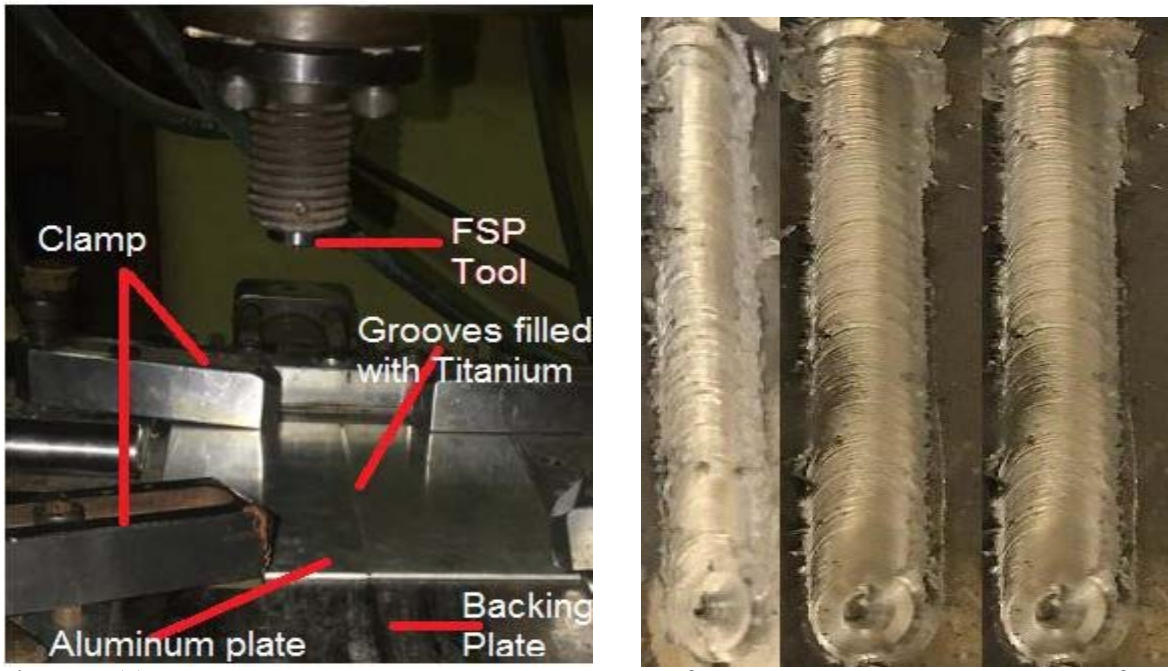

Figure 2 (a) 5-*axis FSW machine which is developed for FSP. (b) Crown appearance of the samples*

High speed steel (HSS) is employed as the tool used for the FSP, even distribution of the Ti-6Al-4V particles in the base material and required frictional heat is attained by this tool. The tool geometries used include square and threaded taper, which has shoulder width of 20 mm and pin length of 4mm with a pin width of 4 mm as shown in Figure 3a and 3b, these tool geometries were chosen due to their frequent use in FSP and their good performance in stirring reinforcement particles [34]., three different passes of FSP was employed with two different tool geometries and two different tool rotational speed. Excessive number of passes may generate inadequate and excessive heat input which in turn will create an adverse effect on the properties of the material that is being processed [35]. The tests were conducted with a tool rotational speed of 600 and 1200rpm, and 10mm/min plunge speed with a constant traverse speed of 30 mm/min. Twelve different composite samples (designated as A1, A2, A3, B1, B2, B3, X1, X2, X3, Y1, Y2 and Y3) were produced. Table 3 shows the definition of symbols for every combination of parameters. To produce an accurate experimental data, two replicates were fabricated for each sample.

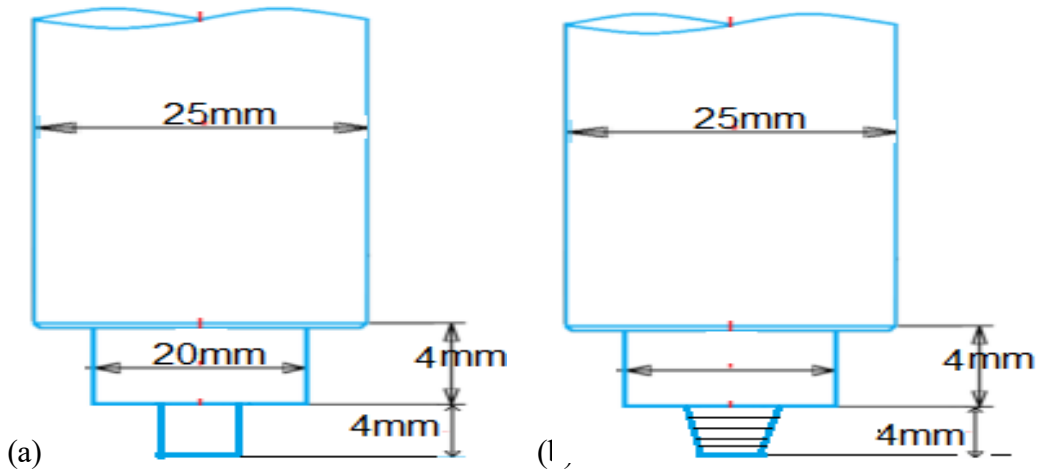

Figure 3: Tool-pin geometry employed in the present study (a) Square (b) Threaded Taper

Table 3: Definition of symbols

Composites	Tool Geometry	Passes	RPM	Fixed Parameters
A	Threaded	1	600	Feed rate (f): 30 mm/min.
1	Threaded	2	600	
A	Threaded	3	600	Tilt angle (α): 2.51.
2				
A	Threaded	1	1200	Shoulder penetration (d)
3	Threaded	2	1200	0.2mm.
	Threaded	3	1200	
B1				Plunge speed 10mm/min.
B2	Square	1	600	
B3	Square	2	600	Inter-pass overlap: 100% .
	Square	3	600	
X				
1	Square	1	1200	
X	Square	2	1200	
2	Square	3	1200	

All samples were cut through a precision metallographic cutting machine in order to measure the micro-hardness and also to observe the particles distribution across the cross section of the samples. These samples were mounted in the thermoset resin and subsequently polished to a mirror-like finishing. Different lines of indentations were made from the top to the bottom surface of the sample and Vicker's microhardness tests were carried out by means of a digital microhardness tester with diamond indenter in accordance to ASTM E92-82 [36] standard by using 300 KN load and 15 seconds dwell time. The samples were degreased with acetone and grinded with an abrasive paper to obtain a smoother surface before taking measurements on the top surface. Metallographic observations and Energy-dispersive X-ray spectroscopy (EDS) microanalyses were conducted to evaluate the dispersion of the Titanium

powders within the aluminium. A TESCAN Scanning Electron Microscope (SEM) equipped with Oxford instrument was used to analyse the distribution of the particle and surface morphology at high magnification. The wear performance of composites and as-cast 1100 Al were tested by conducting pin-on-disc tests. In the present study, the following parameters were fixed during the wear test pin =6 mm; pin =5mm,60HV as the average hardness value of the steel disc and 0.2 μm surface roughness; 17.5 mm as the disc radius; wear radius is13.5 mm; acquisition rate 100Hz; 1000m as the sliding distance; sliding speed is 4.19cm/s; 20N normal load, Relative humidity of 50%. Before the wear tests were carried out, each sample were ground with abrasive paper of 1000 micron. All the tests were done at 50% relative humidity and at the room temperature (25° C). Profilometer was used to measure the mass loss of each sample after the test and the worn surfaces was studied with the use of SEM and EDS. Tensile tests were done at room temperature (25 ºC) via an Instron electronic tensile machine, which has a strain rate of $2.0\times10-3\ s^{-1}$. The samples used for the tensile test were prepared as per ASTM standard E8/E8M-11 as shown in figure 4 and the fracture mode was observed with SEM at the fracture surface.

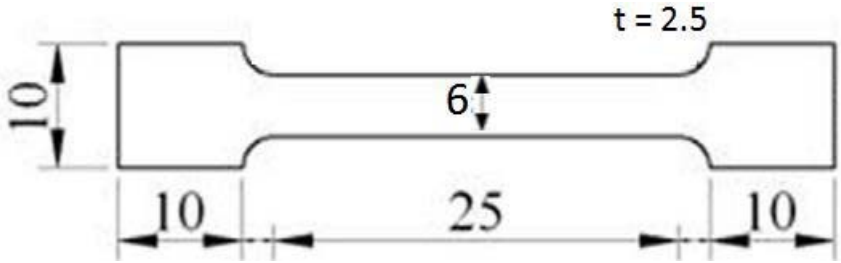

Fig 4: Dimension of Tensile sample

Results and Discussion

Microstructural Analysis of The Al/Ti-6Al-4V Surface Composites

The optical micrographs of various composite samples are presented in Fig 4. As revealed in these figures, A1, X1, Y1 and B1 samples suffer from defects such as tunnel hole, particle agglomeration and pin hole, but A3 and B3 samples are defects free. However, the samples fabricated with square tool geometry on tool speed of 1200rpm with multi passes were damaged (i.e Y2, Y3). The result indicates that the 3—passes samples fabricated via threaded tool experiences better distribution of particles than samples with 1 and 2-passes FSP. This findings can be attributed to the improved stirring action that occurs as the passes increases [37]

.

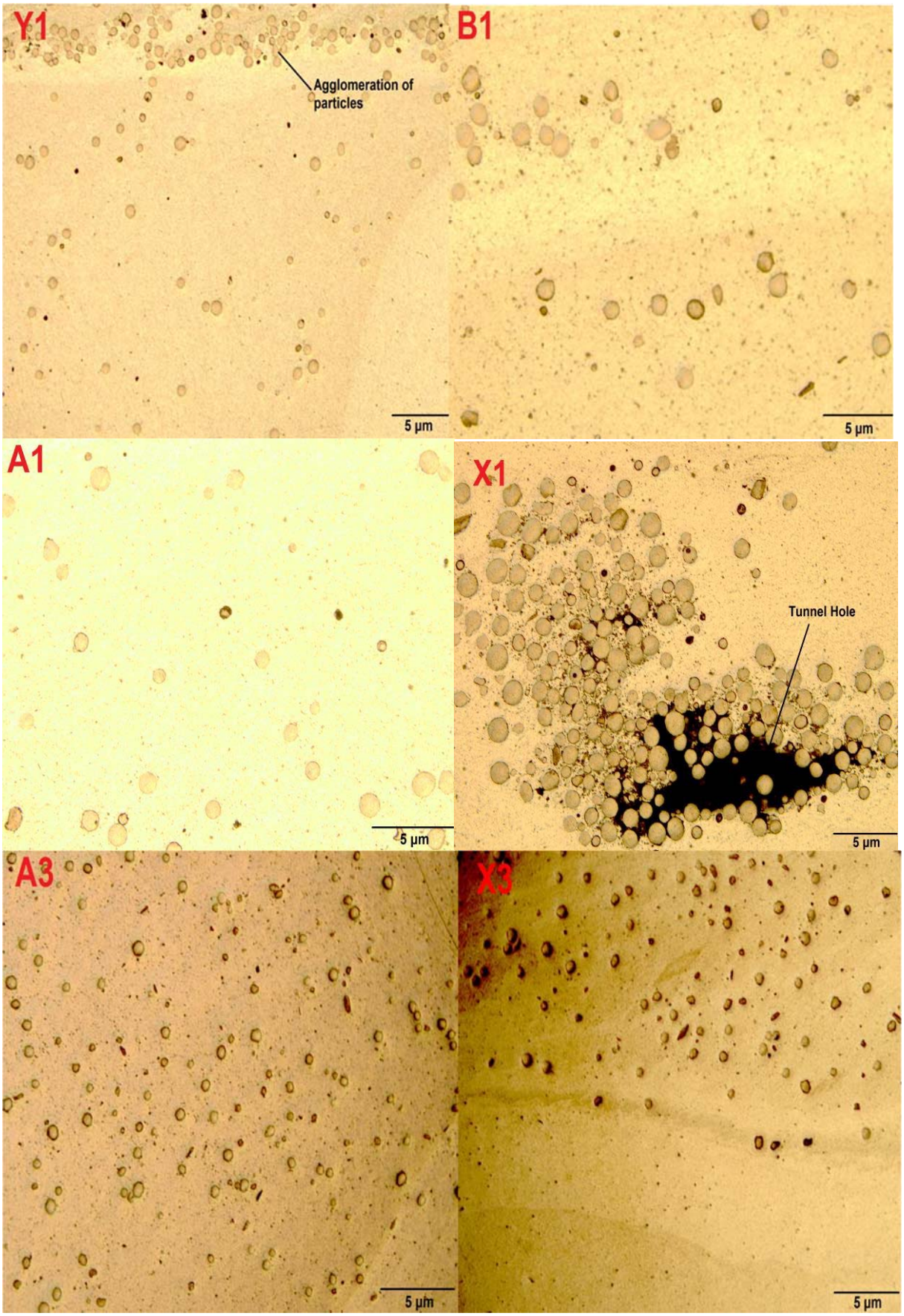

Fig 4: Optical Micrograph of various composites samples

The SEM micrographs of some samples are presented in figure 5 which shows the distribution of the Ti-5Al-4V powder in some selected samples. From these images, it can be seen that the Ti-6Al-4V powder is well distributed in the 3 passes samples (i.e A3, B3, X3) except for the 3-passes fabricated via square tools with 1200rpm (i.e. Y3). In addition, the best particle distribution is shown by the B3 sample which was fabricated using the threaded tool with tool rotational speed of 1200rpm. It is observed in Fig 5, the A3 and B3 samples has white area all through their stir zones (The presence of Ti-6Al-4V particles are represented by the white area), this finding reveals that the reinforcement is properly distributed by the threaded tools on both 600 and 1200 rpm with 3 passes. On the contrary, the stir zones of other samples reveal lesser distribution of Ti-6Al-4V particles; these observations reveal that the threaded tools on 3 passes give better distribution of particles in comparison to the square tool.

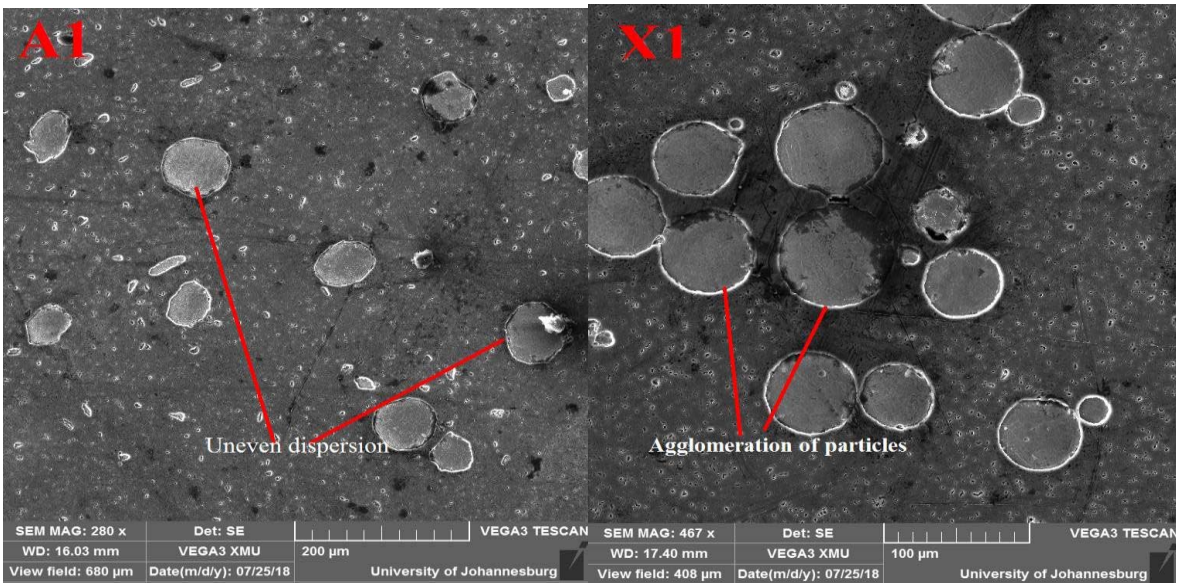

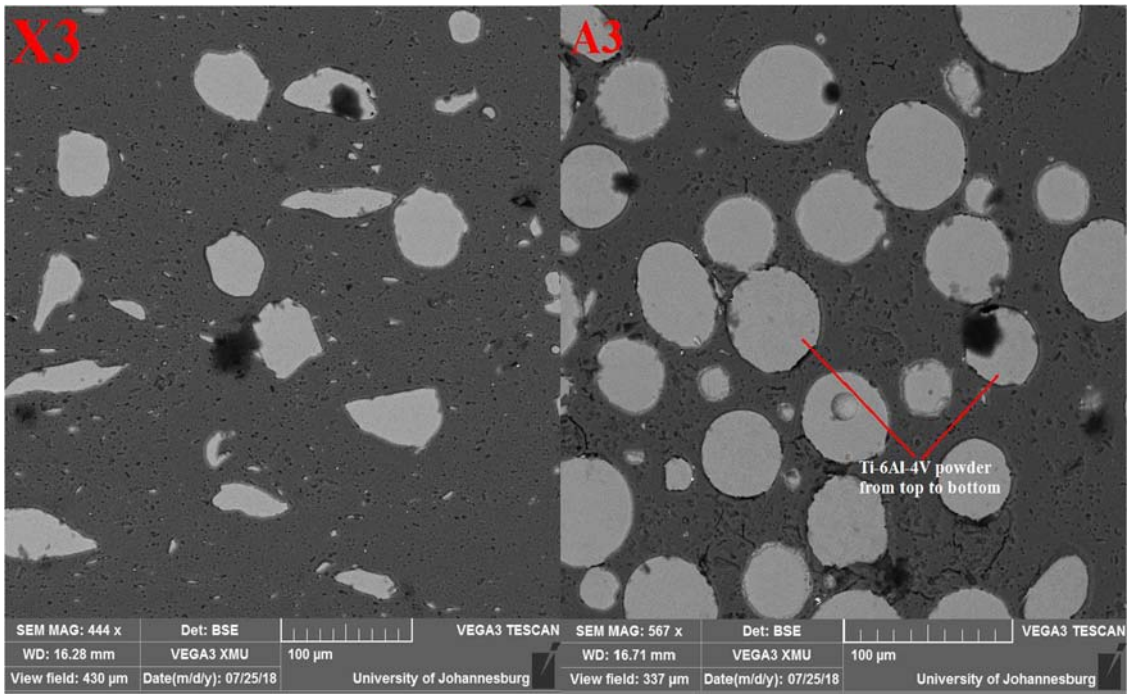

Fig 5: Distribution of Ti-6Al-4V powder within the matrix of some composites samples

Some samples produced with square tool geometry with 1200rpm (i.e Y2 and Y3) were damaged as shown in Figure 6, this is due to inadequate heat input as a result of the tool rotational speed combined with square tool geometry.

Fig 6: Damaged sheet and tool fabricated with 3-passes Square tool geometry with 1200rpm

Hardness measurement and Tensile properties

The hardness value has a 41% increment in the composite when compared to the 1100 Al alloy, a uniform hardness of 26.51 HV is seen across the cross section of the base. The hardness of the processed zone shows a noticaeble variation, small hardness values are seen in the advancing side while the retreating sides show slightly increased hardness value. The titanium particles are accumulated more at the retreating side and the accumulated particles are the reasons for the increased hardness evident in the retreating side of the processed zone

The mean hardness values for all samples are reported in figure 9, tt can be seen that all the 3-passes samples produced via threaded tools and the 3-passes samples fabricated through square with lower tool speed (i.e A3, B3, X3) exhibit higher hardness than the rest. B3 sample has the highest hardness value (i.e., 45.1 HV that is about 41% higher than 26.52HV of the 1100 Al alloy) and figure 9 compare the hardness values of reinforced Al matrix with the pure Al alloy

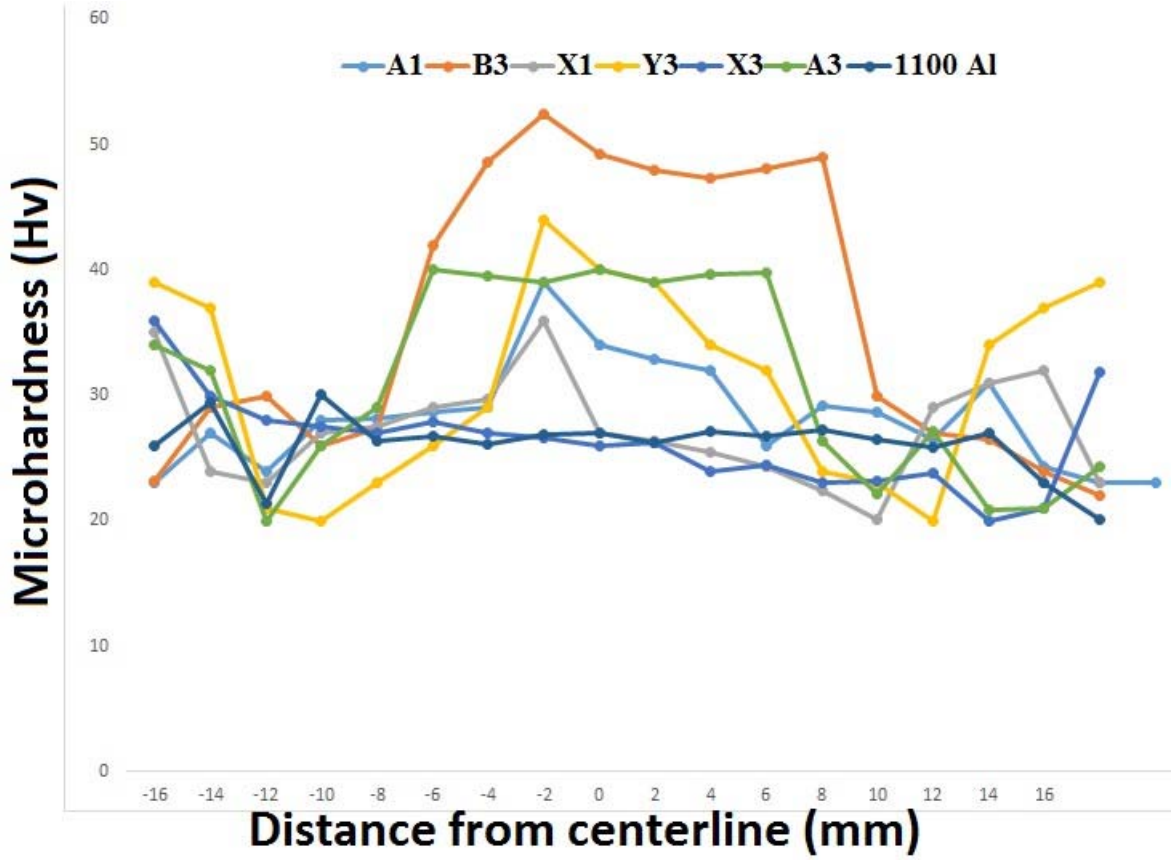

Figure 9: Micro hardness profile of 1100 Al and composite samples at top surface

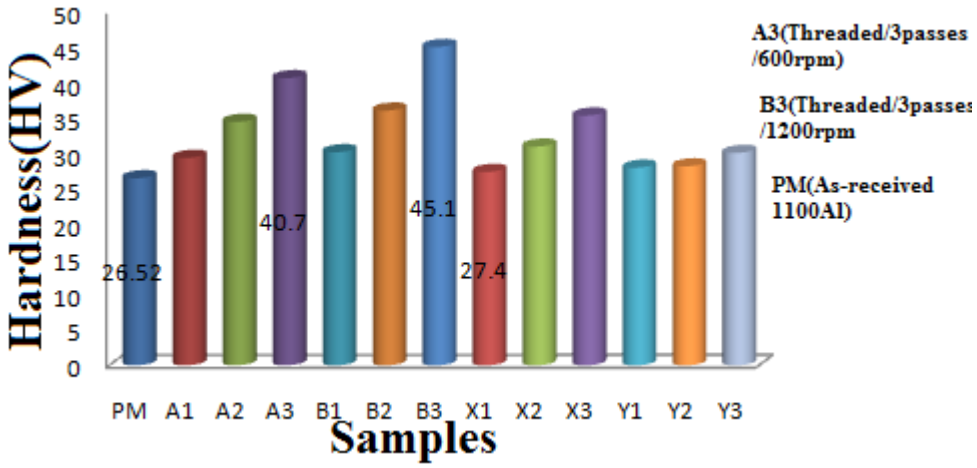

Figure 8: Microhardness of various samples.

The images of the samples before and after test are shown in Fig 10, with a constant sheet thickness of 2.5mm, the load and displacement of all samples were recorded during the test as shown in Figure 11, the samples fabricated with 3-passes showed longer durability and elongation before fracture. The B3 sample being the sample with the highest strength exhibit 30% improvement in tensile strength in comparison with the base metal as shown in Table 4. The yield stress and the Ultimate tensile stress(UTS) of all composite samples are shown in this table. To improve mechanical properties like tensile strength and hardness, it is important to have a better particle refinement according to Hall-Petch rule [37]. In the current work, it can be said that tensile strength increases as the grains in the 1100 Al become more refined, and the tool geometry with the best particle distribution is threaded taper, which further strengthen the need for an appropriate tool geometry when fabricating the Al/Ti-6Al-4V system. The fracture mode of 1100Al alloy and the B3 samples were analysed with SEM as shown in Fig 12, an indication of plastic deformation before failure was revealed due to the dimpled structures observed at the fracture surfaces of these samples. Ductile failure is predicted as the cause of these numerous deformed dimples seen at the surface which is in agreement with the result gotten from the tensile test.

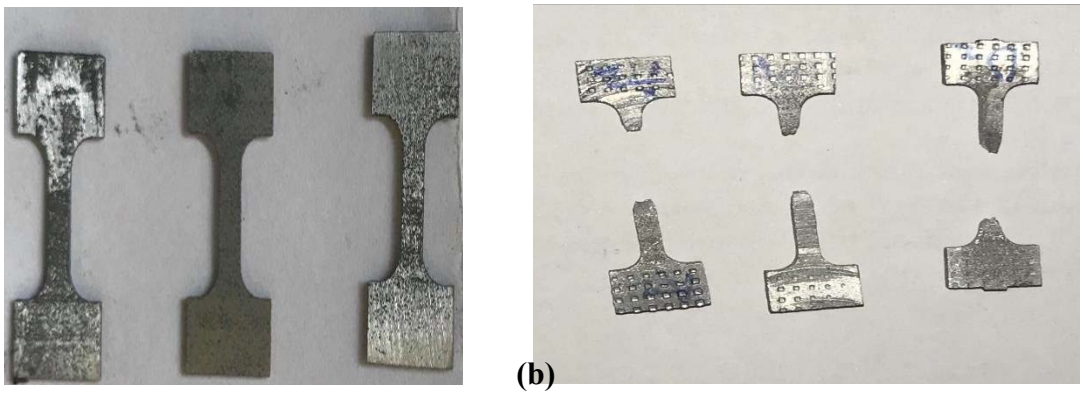

Fig 10: (a) Images of tensile samples before test (b) Images of tensile samples after test

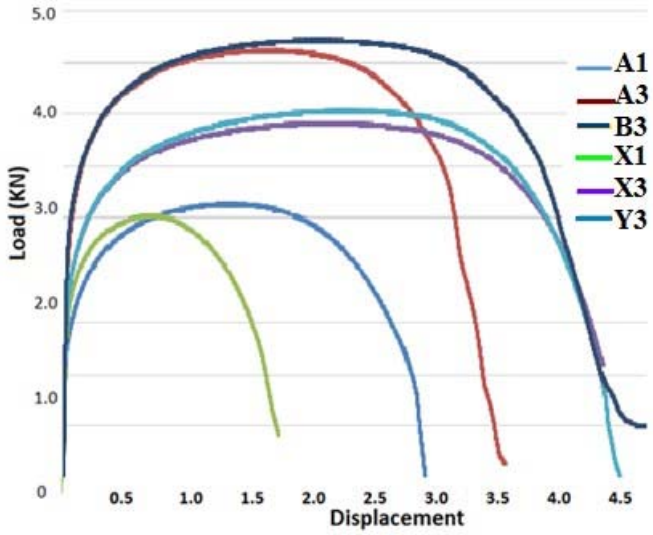

Fig 11: Load- Displacement curves for all composite samples

Table 4. Tensile properties of the composite samples and the 1100Al alloy.

Samples	Yield stress(MPA)	Ultimate Tensile Stress(MPA)	Elongation (%)
1100 Al (PM)	38.16	92.44	34.00
A1	44.66	91.71	43.57
B3	79.78	125.40	66.12
X1	36.51	88.20	40.57
A3	58.90	102.38	51.83
X2	32.85	80.42	32.26
X3	60.11	97.69	54.53

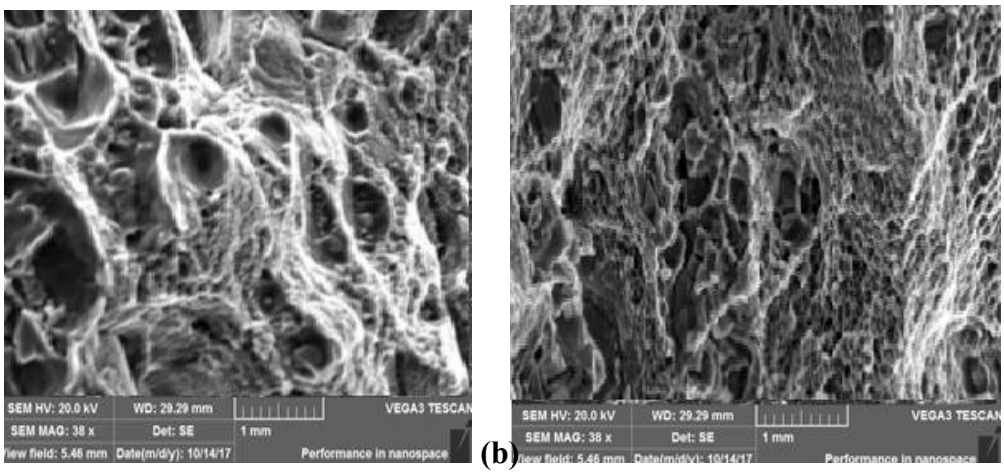

(a) **(b)**

Fig 12: Tensile fracture surfaces (a) 1100Al (b) A2 composite sample

Wear and Friction Performance

Figure 9 presents the coefficient of friction of some selected samples, a noticeable fluctuation occurs in the base metal and samples fabricated via 1-pass. For 3-passes samples produced with threaded tool, a lower and stable friction coefficient was observed all through the test. This means the A3 and B3 composites (both 3-passes produced with threaded tools with different tool speed) can exhibit longer service life. The rest of the samples as shown in figure 9 exhibit different behaviour during the test, they have higher friction compared to A3 and B3 samples. The average coefficient of friction of all samples under 20N load is shown in figure 10, the findings show that the samples produced using 3 passes (i. e., A3, B3, X3) give lower friction coefficient in comparison with samples fabricated using 1 and 2passes (i.e.B1, A1 and the rest). The reason is because the 3-passes samples has better hardness and finer grains in comparison to the rest except for 3- passes fabricated via Square tool geometry that has high tool speed which led to the damage of the sheets due to high heat input. In consistent with Hall–Petch rule, B3 sample exhibit the least friction due to the tool geometry and the high heat input which helps with the stirring of the particles in the 1100Al alloy, and Y1 sample has the highest friction. The friction coefficient of A3 and B3 samples are about 45% lower than that of the as-received 1100 Al. Further, as shown in figure 10

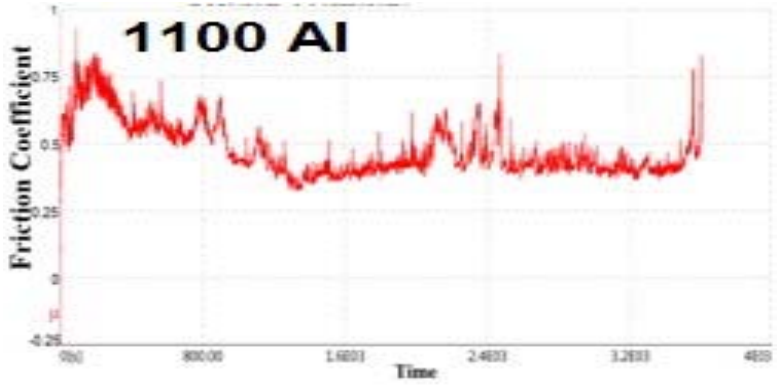
1100 Al
Friction Coefficient
Time

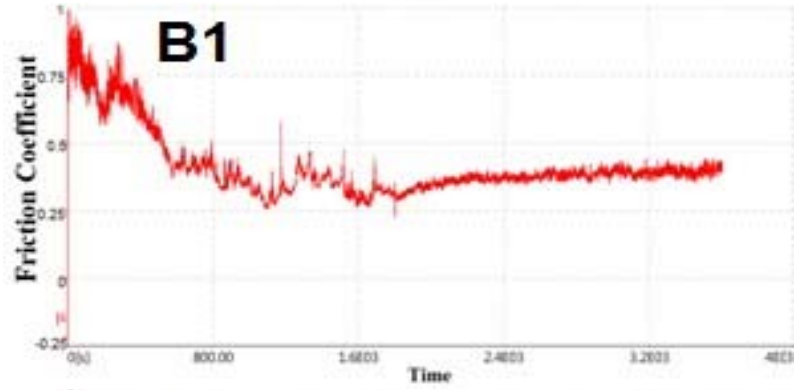
B1
Friction Coefficient
Time

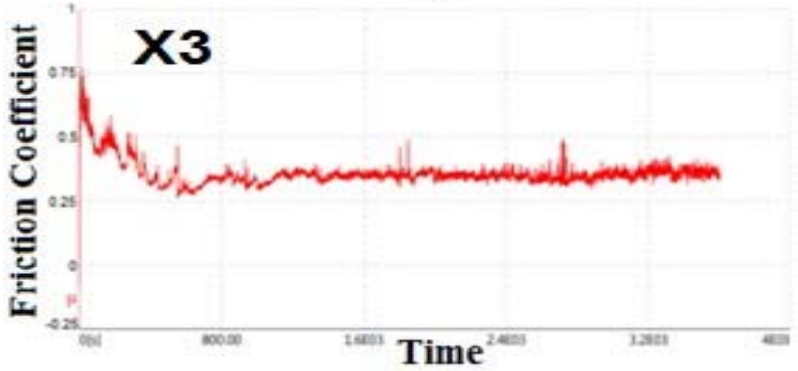
X3
Friction Coefficient
Time

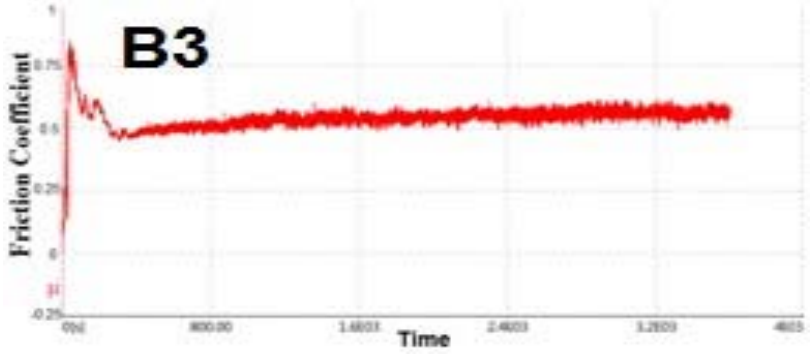
B3
Friction Coefficient
Time

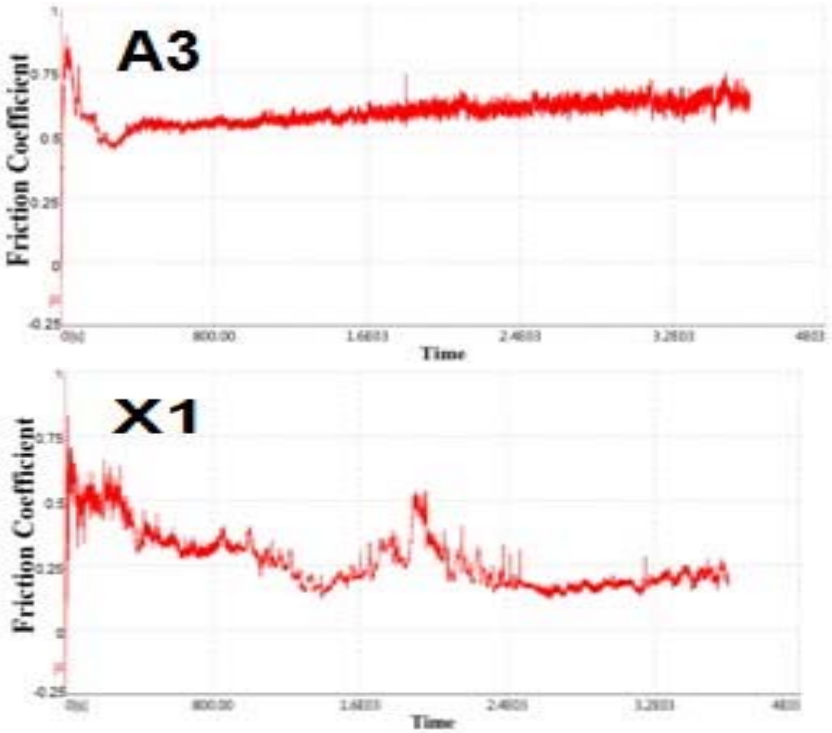

Figure 9: Friction behaviour of 1100 Al alloy and various composite samples (All the samples were tested under normal load of 20N)

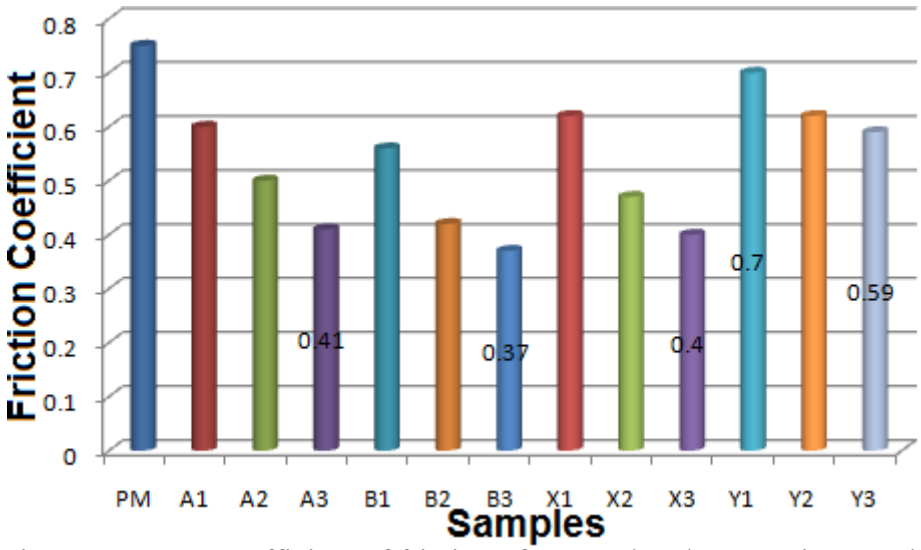

Fig 10: Average coefficient of friction of 1100 Al and composite samples (All the samples were tested under normal load of 20N)

Mass loss of the samples were investigated during the wear test, figure 11 shows the average mass loss of the composite samples. Low loss of mass is evident with the 3-passes samples in comparative to the rest except for Y3 (i.e 3-passes fabricated with square tool geometry and 1200rpm). Furthermore, the hardest composite samples being B3 experience the least mass loss, which is about 67% lower than the mass loss of the 1100 Al alloy. This

finding shows that the addition of 25% volume of Ti-6Al-4V particles may improve the wear performance of aluminium alloy by 67%. Furthermore, due to the performance exhibited by B3 samples in terms of hardness, resistance to wear, distribution of particles and finer grains, the importance of using the combination of 3-passes, 1200rpm and threaded tool to fabricate Al/Ti-6Al-4V composite can be overemphasised.

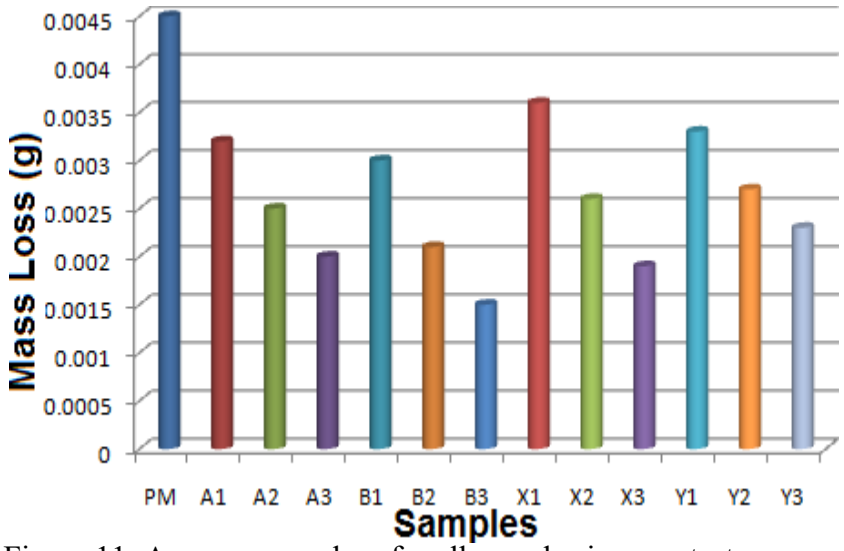

Figure 11: Average mass loss for all samples in wear test

3.4. Worn Surfaces and Comparison Between Reinforced and the Unreinforced Matrix

SEM micrographs of the 1100Al alloy and B3 are shown in figure 12, B3 being the composite with lowest loss of mass and highest hardness has striations on the surface during the test, the present of these striations in B3 suggest abrasive wear. The EDS analysis of the B3 sample is shown in figure 13, it can be seen from the EDS peaks that the composite consists of elements present in the base metal such as Al, Ti and N, which show that the composite experienced adhesion wear. These findings confirm that the composites are controlled by both adhesion and abrasion mechanism.

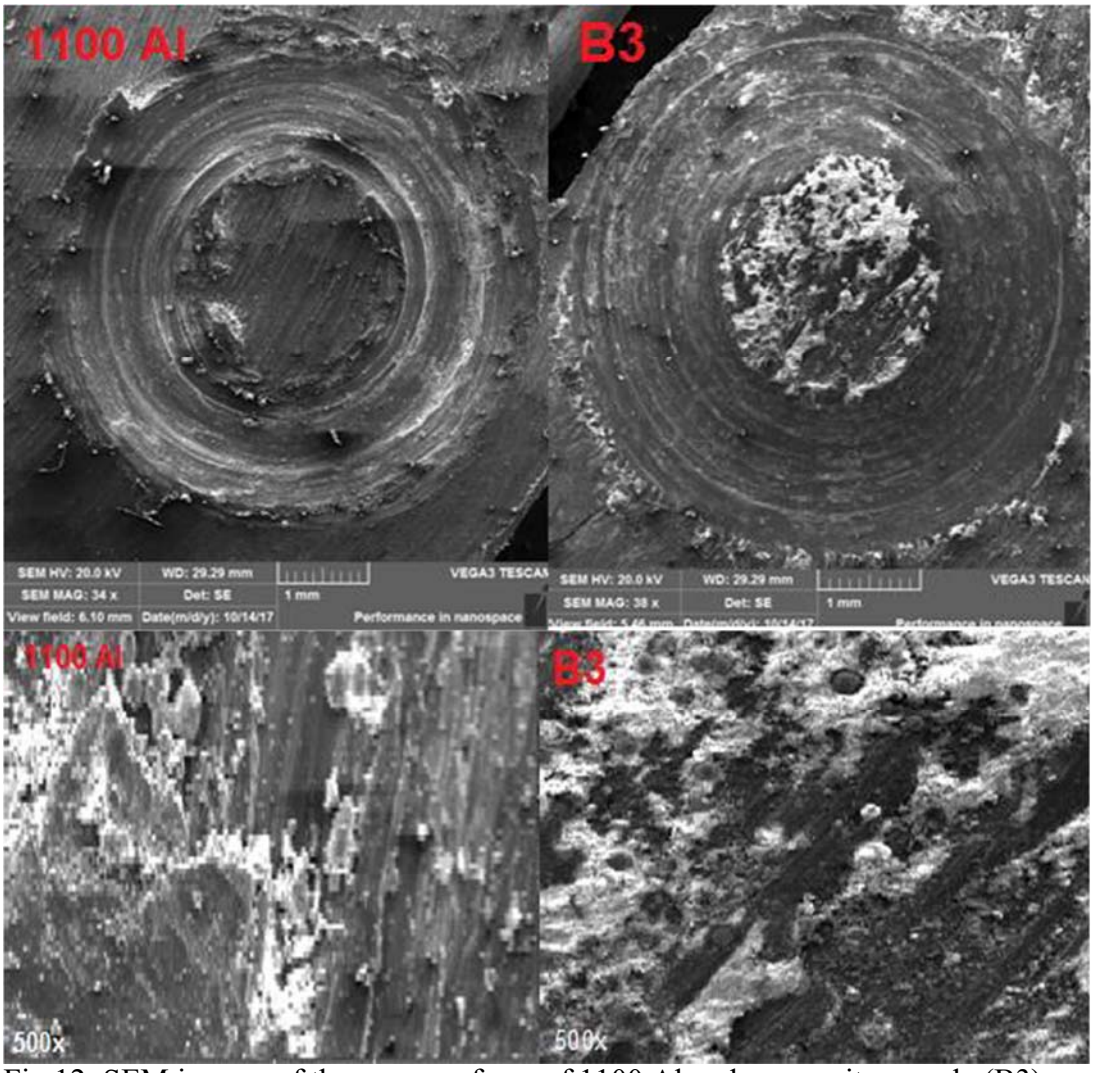

Fig 12: SEM images of the worn surfaces of 1100 Al and composite sample (B3)

The surface of B3 was analysed via EDS as shown in figure 13, Two zones were selected (A and B). The EDS peaks at zone A has in present Al_2Ti intermetallic and zone B represents the existence of Titanium rich particles. These observations are due to tribo- reactions which help to prevent contact between disc and composite material which subsequently alters the wear mechanism by making it a reaction between three bodies, consequently improving the resistance to wear of the composite sample. It can be concluded that in the fabrication of the Al-Ti-6Al-4V system, the wear resistance may also be affected by tribo growth.

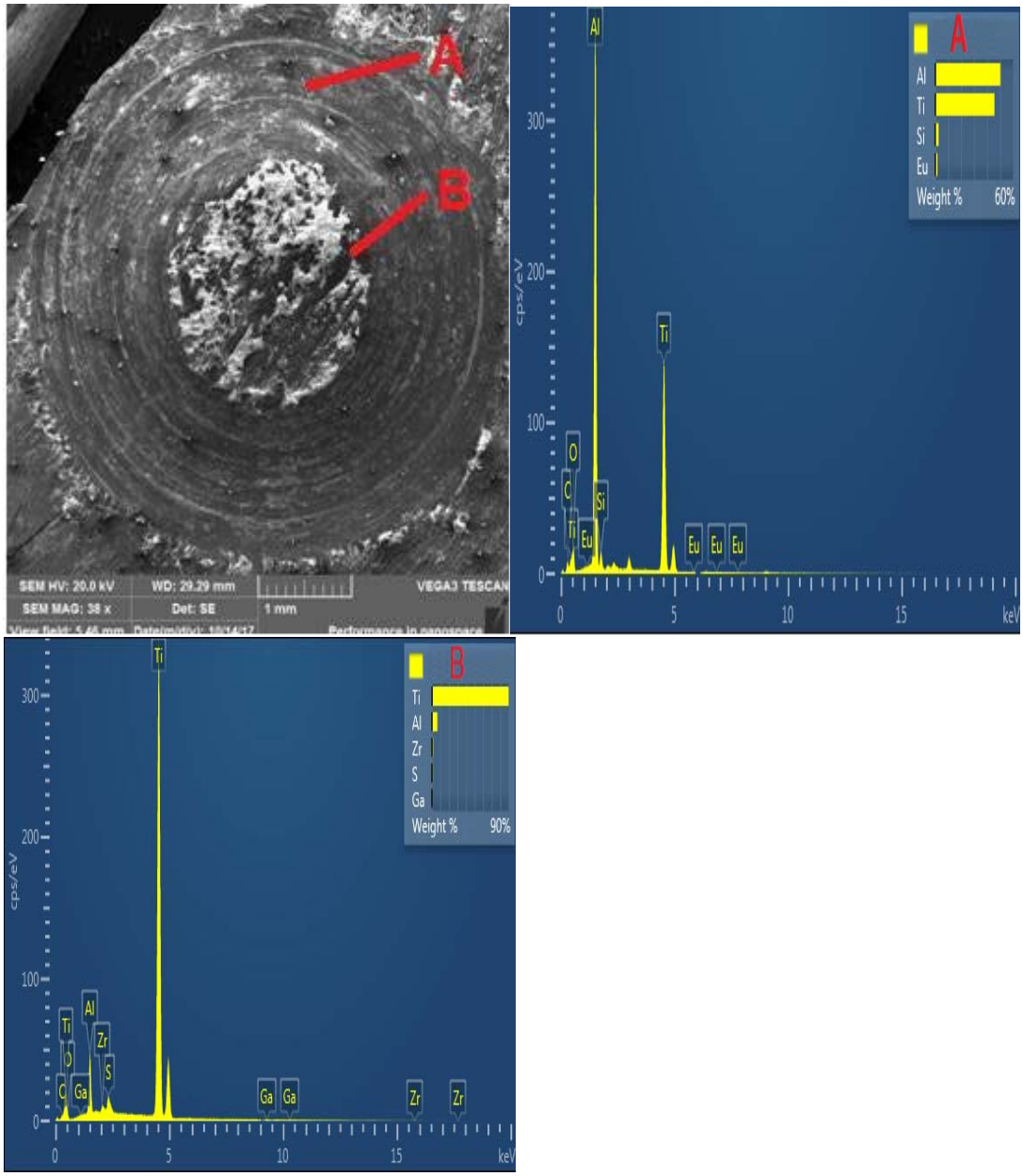

Fig 13: EDS analysis of the worn surface of B3

The mass loss and hardness value for composite with the highest hardness (i.e B3) is compared with 3-pass sample without reinforcement and the 1100 Al alloy in Table 4. Threaded tool was used to fabricate the unreinforced 3-passes sample. It can be seen in Table 4 that the 1100 Al alloy has higher hardness than the unreinforced 3 passes sample, and the highest hardness being B3 (3-passes composite sample). The mass loss also follow similar trend, the mass loss of the unreinforced 3 passes sample is the highest which is as a result of the annealing effect of the heat generated during the process. This study shows that all the properties such as friction coefficient, mass loss and the hardness value of the reinforced 3- passes composite(B3) performs better than the unreinforced 3-passes sample, and this finding shows that the Ti-6Al-4V particles can prevail over the annealing effect of the heat generated during the process In

summary, the effects of number of passes, tool rotational speed and the tool geometry in fabricating the Al/Ti-6Al-4V surface composite can be seen on the hardness, grain size, particle distribution of particles and the resistance to wear of the composite. The best choice for fabricating this surface composite is the combination of 3-passes with threaded tool and a tool speed of 1200rpm.

Table 4: Hardness and wear resistance of parent material, reinforced and unreinforced 1100 Al

Attribute	Parent Material	Unreinforced/3passes	3-passes composite(B3)
Mass loss(g)	0.0045	0.0051	0.0014
Hardness(HV)	26.52	23.6	45.1
Coefficient of Friction	0.75	0.056	0.36

Conclusion

This research was done with the aim to improve the mechanical properties of 1100 Al alloy. Tool parameters such as number of passes, tool rotational speed and tool geometry were examined to find the most suitable combination offering an even distribution of the powder which in turn affects the hardness, tensile property and the wear resistance of the composite. The conclusions of this research are summarized below.

1 The wear resistance of 1100 Al Alloy can be enhanced by reinforcing it with Ti-6Al-4V particles. A decrease in the friction coefficient and an appreciable increase in the wear resistance due to the addition of the powder as reinforcement was observed in this study.

2. The more even the dispersion, the higher the wear resistance, and as the passes increases, the distributions of the particles are more even. Furthermore, the particle distribution is affected by the tool geometry and the tool rotational speed, a higher tool speed which produces more heat input helps in dispersing the powder uniformly. In the present work, the resistance to wear of the 1100 Al alloy is dependent on how uniformly the Ti-6Al-4V are distributed in the matrix.

3. Threaded taper tool geometry is the most suitable tool among the tools in this research to fabricate Al/Ti-6Al-4V surface composite, the best particle distribution is gotten from 3- passes composites produced with threaded tool and tool speed of 1200rpm. With this combination, 30% improvement in tensile strength was recorded in comparison with the 1100 Al alloy.

4. It was observed in this research that microstructural modifications occur as the passes increases, modifications such as breakup of acicular Ti particles, pitholes and elimination of

defects. A finer and better distribution with less agglomeration can be seen as the passes increases.

Acknowledgements

The authors are grateful to Mechanical Engineering Department of India Institute of Science, Bangalore India for the experimental work carried out in their Laboratory, also grateful to the University of Johannesburg for characterizations done at the Materials Laboratory

References

[1] O. S. Salih, H. Ou, W. Sun, and D. G. Mccartney, "A review of friction stir welding of aluminium matrix composites," *JMADE*, vol. 86, pp. 61–71, 2015.

[2] R. S. Mishra, Z. Y. Ma, and I. Charit, "Friction stir processing: A novel technique for fabrication of surface composite," *Mater. Sci. Eng. A*, vol. 341, no. 1–2, pp. 307–310, 2003.

[3] I. Journal *et al.*, "A Review on Properties, Behaviour and Processing Methods for Al-Nano Al2O3 Composites," *Procedia Eng.*, vol. 97, no. 4, pp. 24–27, 2017.

[4] F. Khodabakhshi, A. P. Gerlich, and P. Š, "Materials Science & Engineering A Fabrication of a high strength ultra- fi ne grained Al-Mg-SiC nanocomposite by multi-step friction-stir processing," vol. 698, no. May, pp. 313–325, 2017.

[5] V. Sharma, U. Prakash, and B. V. M. Kumar, "Journal of Materials Processing Technology Surface composites by friction stir processing : A review," *J. Mater. Process. Tech.*, vol. 224, pp. 117–134, 2015.

[6] R. Hashemi and G. Hussain, "Wear performance of Al/TiN dispersion strengthened surface composite produced through friction stir process: A comparison of tool geometries and number of passes," *Wear*, vol. 324–325, pp. 45–54, 2015.

[7] A. Rahbar-Kelishami, A. Abdollah-Zadeh, M. M. Hadavi, R. A. Seraj, and A. P. Gerlich, "Improvement of wear resistance of sprayed layer on 52100 steel by friction stir processing," *Appl. Surf. Sci.*, vol. 316, no. 1, pp. 501–507, 2014.

[8] D. K. Koli, G. Agnihotri, and R. Purohit, "A Review on Properties, Behaviour and Processing Methods for Al- Nano Al2O3 Composites," *Procedia Mater. Sci.*, vol. 6, no. Icmpc, pp. 567–589, 2014.

[9] S. Chainarong, P. Muangjunburee, and S. Suthummanon, "Friction stir processing of SSM356 aluminium alloy," *Procedia Eng.*, vol. 97, pp. 732–740, 2014.

[10] U. Pandey, R. Purohit, P. Agarwal, and S. Kumar Singh, "Study of Fabrication, Testing and Characterization of Al/TiC Metal Matrix Composites through different Processing Techniques," *Mater. Today Proc.*, vol. 5, no. 2, pp. 4106–4117, 2018.

[11] A. Suri, A. Sahai, K. H. Raj, and N. K. Gupta, "Impact and Tensile testing of Al2024 Alloy Processed by Friction Stir Processing," *Procedia Eng.*, vol. 173, pp. 679–685, 2017.

[12] D. Ahmadkhaniha, M. Heydarzadeh Sohi, A. Salehi, and R. Tahavvori, "Formations of AZ91/Al2O3 nano-composite layer by friction stir processing," *J. Magnes. Alloy.*, vol.

4, no. 4, pp. 314–318, 2016.
[13] A. Smolej *et al.*, “Superplasticity of the rolled and friction stir processed Al-4.5 Mg-0.35Sc-0.15Zr alloy,” *Mater. Sci. Eng. A*, vol. 590, pp. 239–245, 2014.
[14] H. Izadi, A. Nolting, C. Munro, D. P. Bishop, K. P. Plucknett, and A. P. Gerlich, “Journal of Materials Processing Technology Friction stir processing of Al / SiC composites fabricated by powder metallurgy,” *J. Mater. Process. Tech.*, vol. 213, no. 11, pp. 1900–1907, 2013.
[15] M. Azizieh, D. Iranparast, M. A. G. Dezfuli, Z. Balak, and H. S. Kim, “Fabrication of Al / Al 2 Cu in situ nanocomposite via friction stir processing,” *Trans. Nonferrous Met. Soc. China*, vol. 27, no. 4, pp. 779–788, 2017.
[16] S. Dodds, A. H. Jones, and S. Cater, “Tribological enhancement of AISI 420 martensitic stainless steel through friction-stir processing,” *Wear*, vol. 302, no. 1–2, pp. 863–877, 2013.
[17] D. Khayyamin, A. Mostafapour, and R. Keshmiri, “Materials Science & Engineering A The effect of process parameters on microstructural characteristics of AZ91 / SiO 2 composite fabricated by FSP,” *Mater. Sci. Eng. A*, vol. 559, pp. 217–221, 2013.
[18] Y. CHEN, H. DING, S. MALOPHEYEV, R. KAIBYSHEV, Z. CAI, and W. YANG, “Influence of multi-pass friction stir processing on microstructure and mechanical properties of 7B04-O Al alloy,” *Trans. Nonferrous Met. Soc. China*, vol. 27, no. 4, pp. 789–796, 2017.
[19] G. Wang *et al.*, “Effects of weld reinforcement on tensile behavior and mechanical properties of 2219-T87 aluminum alloy TIG welded joints,” *Trans. Nonferrous Met. Soc. China*, vol. 27, no. 1, pp. 10–16, 2017.
[20] M. Ramosoeu *et al.*, “Tribological enhancement of AISI 420 martensitic stainless steel through friction-stir processing,” *Wear*, vol. 27, no. c, pp. 779–788, 2013.
[21] J. Kemmler, S. O. Schopf, L. Mädler, N. Barsan, and U. Weimar, “New process technologies for the deposition of semiconducting metal oxide nanoparticles for sensing,” *Procedia Eng.*, vol. 87, pp. 24–27, 2014.
[22] F. Abraham, “Tensile properties and fracture behaviour of Multipass Friction Stir Processed Al-7Si-0 . 3Mg cast alloy by,” no. July, 2012.
[23] M. Golmohammadi, M. Atapour, and A. Ashra, “Fabrication and wear characterization of an A413 / Ni surface metal matrix composite fabricated via friction stir processing,” vol. 85, pp. 471–482, 2015.
[24] M. Ramosoeu, H. Chikwanda, A. Bolokang, G. Booysen, and T. Ngonda, “Additive manufacturing: Characterization of TI-6AI-4V alloy intended for biomedical application,” *South. African Inst. Min. Metall. Adv. Met. Initiat. Light Met. Conf.*, no. c, pp. 337–344, 2010.
[25] Y. M. Ahmed, K. Salleh, M. Sahari, M. Ishak, and B. A. Khidhir, “Titanium and its Alloy,” no. May 2015, 2014.
[26] R. Pederson, “Microstructure and Phase Transformation of Ti-6Al-4V,” 2002.
[27] B. S. Li, J. L. Shang, J. J. Guo, and H. Z. Fu, “In situ observation of fracture behavior of in situ TiB w / Ti composites,” vol. 383, no. April, pp. 316–322, 2004.
[28] P. Vijayavel and V. Balasubramanian, “Effect of pin profile volume ratio on microstructure and tensile properties of friction stir processed aluminum based metal matrix composites,” *J. Alloys Compd.*, vol. 729, pp. 828–842, 2017.
[29] S. Rathee, S. Maheshwari, A. N. Siddiquee, and M. Srivastava, “Effect of tool plunge depth on reinforcement particles distribution in surface composite fabrication via friction stir processing,” *Def. Technol.*, vol. 13, no. 2, pp. 86–91, 2017.
[30] E. Nyoni and E. T. Akinlabi, “Process parameter interaction effect on the evolving properties of laser metal deposited titanium for biomedical applications,” *Thin Solid*

Films, vol. 620, pp. 94–102, 2016.
[31] A. Arora, A. Astarita, L. Boccarusso, and V. P. Mahesh, "Experimental Characterization of Metal Matrix Composite with Aluminium Matrix and Molybdenum Powders as Reinforcement," *Procedia Eng.*, vol. 167, pp. 245–251, 2016.
[32] M. E. Maja, O. E. Falodun, B. A. Obadele, S. R. Oke, and P. A. Olubambi, "Nanoindentation studies on TiN nanoceramic reinforced Ti – 6Al – 4V matrix composite," *Ceram. Int.*, vol. 44, no. 4, pp. 4419–4425, 2018.
[33] A. Thangarasu, N. Murugan, and I. Dinaharan, "Production and wear characterization of AA6082-TiC surface composites by friction stir processing," *Procedia Eng.*, vol. 97, pp. 590–597, 2014.
[34] N. Nadammal, S. V. Kailas, and S. Suwas, "A bottom-up approach for optimization of friction stir processing parameters; a study on aluminium 2024-T3 alloy," *Mater. Des.*, vol. 65, 2015.
[35] M. Rahsepar and H. Jarahimoghadam, "The influence of multipass friction stir processing on the corrosion behavior and mechanical properties of zircon-reinforced Al metal matrix composites," *Mater. Sci. Eng. A*, vol. 671, pp. 214–220, 2016.
[36] N. Saini, D. K. Dwivedi, P. K. Jain, and H. Singh, "Surface modification of cast Al-17%Si alloys using friction stir processing," *Procedia Eng.*, vol. 100, no. January, pp. 1522–1531, 2015.
[37] M. Moghaddam *et al.*, "Materials Characterization Characterization of the microstructure , texture and mechanical properties of 7075 aluminum alloy in early stage of severe plastic deformation," *Int. J. Fatigue*, vol. 119, pp. 192–202, 2016.